Proceedings of the 3rd IEEE Int. Conf. on
Nano/Micro Engineered and Molecular Systems
January 6-9, 2008, Sanya, China

Manipulating Nanoparticles and Macromolecules with Light Patterned Microfluidic Flow

P. Y. Chiou, *Member, IEEE*, and M. C. Wu, *Fellow, IEEE*

[1] *Mechanical and Aerospace Engineering Department, University of California at Los Angeles,, USA*
[2]*Electrical Engineering and Computer Sciences Department, University of California at Berkeley, USA*

***Abstract*— We present a novel light-actuated ac electroosmosis (LACE) mechanism allowing concentrating and transporting micro-, nano-scale particles including macromolecules using light-patterned, dynamically reconfigurable microfluidic vortices on a photoconductive surface. LACE is realized by sandwiching an aqueous liquid medium between a featureless photoconductive surface and a transparent ITO electrode. Under the application of an ac bias with a frequency close to the electric double layer relaxation frequency, a light beam can create a microfluidic vortex flow around the illuminated area through ac electroosmosis. By integrating with a spatial light modulator such as a DMD microdisplay, LACE allows the creation of 31,000 microfluidic vortices on a 1.3 × 1 mm2 area for massively parallel trapping of 2-μm, 1 μm, 500 nm, 200 nm, and 50 nm polystyrene beads. We have also demonstrated LACE concentration and transportation of λ-phage DNA molecules, and quantum dots.**

Keywords: *ACEO, Electroosmosis, Optoelectronic Tweezers,OET, DNA manipulation, Dielectrophoresis, Lab-on-a-Chip*

I. INTRODUCTION *(HEADING 1)*

Tools for manipulating cells, micro- and nano-particles are important in the fields of biological and colloid science. Functions such as trapping, concentrating, sorting, and transporting are highly sought of. To effectively manipulate nanoscale particles, strong field strength is necessary to form stable traps to overcome the strong Brownian motions of nanoparticles, especially for the cases of optical tweezers[1, 2], dielectrophoresis (DEP)[3, 4], optoelectronic tweezers[5] and magnetic tweezers[6, 7] that give trap forces proportional to the volume of the trapped particles. When particle size scales down to the nanometer scale, strong fields are needed, and this often imposes limitations on manipulations. For example, a strong optical field could damage a spatial light modulator used for shaping a light beam; a strong electric field used in DEP traps could induce electrolysis that changes the local chemical composition or create joule heating that raises the local temperature.

On the other hand, ac electroosmosis has recently been demonstrated to be capable of manipulating nanoscale particles with low electric field strength. Wong et al. [8] has utilized ac electroosmosis to concentrate a variety of nanoscale particles and biomolecules including *E. Coli* Bacteria, λ-phage DNA and 20-base single-strand DNA fragments with electric field strength on the order of 10^4 V/m.

This project is supported in part by supported by the Center for Cell Mimetic Space Exploration (CMISE), a NASA University Research, Engineering and Technology Institute (URETI), and the Graduate Research and Education in Adaptive Bio-Technology (GREAT) training program.
Contact author: Eric Pei-Yu Chiou, University of California at Los Angeles, CA 90095, USA (pychiou@seas.ucla.edu).

In this paper, we present a light-actuated ac electroomosis (LACE) mechanism that allows optically-patterned microfluidic vortices and self-aligned surface electric fields to concentrate and transport nanoparticles continuously on a photoconductive surface. Tens of thousands of microfluidic vortices can be patterned on a 1.3 × 1 mm^2 area for massively parallel manipulation of micro- and nanoscopic particles.

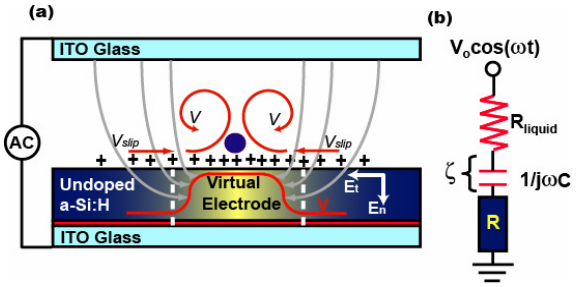

Fig. 1 Illustration of LACE mechanism (a) A microfluidic vortex generated by a light-patterned virtual electrode through driving the double layer charges via the tangential component of electric field. (b) The equivalent circuit model along an electric field line. LACE operates at frequencies close to the double layer relaxation frequency.

II. LIGHT ACTUATED AC ELECTROOSMOSIS

Electroosmosis is widely used in microfluidics for liquid pumping[9-11]. The tangential electric field in a fluidic channel interacts with the charged ions in the double layer and generates an electrostatic force to drive the boundary liquid to flow at a slip velocity that can be calculated using the Helmholtz-Smoluchowski equation[12]

$$v_{slip} = -\frac{\varepsilon \zeta E_t}{\eta} \qquad (1)$$

where v_{slip} is the slip velocity, ε is the permittivity of the liquid medium, ζ is the zeta potential at the interface between the liquid and the channel wall, E_t is the tangential component of electric field, and η is the fluidic viscosity.

Electroosmosis is usually observed in dc mode, in which the zeta potential is determined by the material property of the channel wall, the type of electrolytes, and the ionic strength. Recently, ac electroosmosis has also been applied to generate continuous dc flow by coupling the tangential electric field

with the field-induced double layer charges on electrodes[13, 14].

Fig. 1(a) illustrates the device structure and the working principle of LACE. An aqueous medium containing nanoparticles and molecules of interest is sandwiched between a transparent ITO electrode and a photoconductive electrode coated with multiple featureless layers including a 200-nm ITO, a 50-nm n+ a-Si:H, and a 1-μm undoped a-Si:H. An ac bias is applied to the top and the bottom ITO layers. At areas without light illumination, the undoped a-Si:H has high electrical impedance compared to the liquid medium. The majority of the applied voltage drops across the a-Si:H layer. At illuminated areas, the photoconductivity of the undoped a-Si:H layer increases by several orders of magnitude, which switches the voltage to the interfacial double layer capacitor C and the liquid layer resistor R as shown in Fig. 1(b). By using light patterning to create virtual electrodes, electrode patterns can be changed quickly and efficiently, rendering fixed physical or chemical pattering of the electrodes unnecessary.

Since creating the boundary slip velocity requires both the tangential electric field and the charged ions at the interface, there exists an optimal ac frequency at which the product of the electric field and the interface zeta potential in Eq. (1) reaches maximum. For a frequency much higher than f_{opt}, the capacitor has low electrical impedance and the bulk liquid resistor dominates. This results in a small zeta potential and a small slip velocity. For a frequency much lower than f_{opt}, the impedance of the capacitor is much larger than the bulk liquid layer. The electric field that can penetrate through the double layer is small, resulting in a small tangential electric field. This also yields a small slip velocity. The optimal frequency, $f_{opt}=1/2\pi RC$ (see Fig, 1(b), can be estimated to be

$$f_{opt} = \frac{1}{2\pi}\frac{\sigma}{\varepsilon}\frac{\lambda_d}{L} \qquad (2)$$

where σ is the conductivity of the liquid medium, ε is the permittivity of the liquid, λ_d is the double layer thickness, and L is the gap spacing of the liquid layer. For a LACE device with 100-μm gap spacing, a liquid conductivity of 10 mS/m and a double layer thickness around 10 nm, the estimated f_{opt} is 229 Hz. The actual f_{opt} in LACE is higher than this value since the geometry factor is not considered in this estimation. In current LACE devices, the operation ac frequency is usually between 1 kHz ~ 10 kHz. The liquid conductivity used for LACE operation is between 3 mS/m ~ 10 mS/m.

A microfluidic vortex pattern created by a virtual electrode on a LACE device is illustrated in Fig. 1(a). The charged ions accumulated at the interface are driven toward the center of a virtual electrode by the tangential field on the surface. This pumps the surrounding fluids to circulate around the virtual electrode. The polarity of the ions and electric field shown in Fig. 1(a) represents the situation in a half ac cycle. In the other half cycle, the polarities of both the ions and electric field change, resulting in an electrostatic force driving the fluids to flow in the same direction as in the previous half cycle. Therefore, ac electroosmosis allows an ac electrical signal to generate a dc force to pump fluids continuously in the same direction.

The template is used to format your paper and style the text. All margins, column widths, line spaces, and text fonts are prescribed; please do not alter them. You may note peculiarities. For example, the head margin in this template measures proportionately more than is customary. This measurement and others are deliberate, using specifications that anticipate your paper as one part of the entire proceedings, and not as an independent document. Please do not revise any of the current designations.

III. Simulation of Electric Field and Flow Pattern

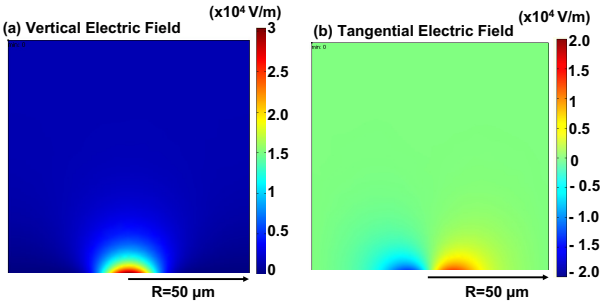

Fig. 2 The vertical and the tangential electric field distribution in the liquid layer induced by a virtual electrode. (a) The vertical component of electric field is symmetrical to the center of a virtual electrode and with its highest field strength in the middle. (a) The tangential component of electric field is anti-symmetric to the center of a virtual electrode and with its highest electric field at the edge of a virtual electrode.

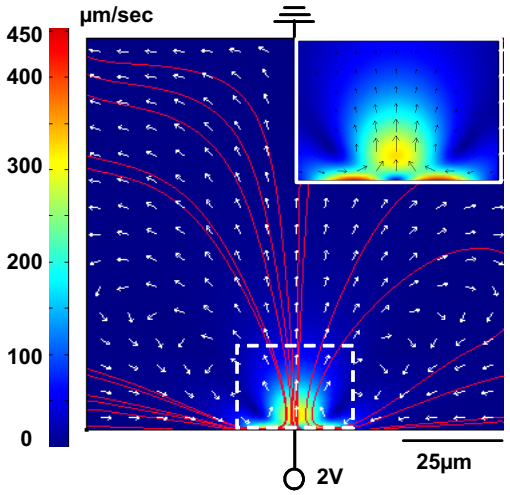

Fig. 3 Light-induced ac electroosmosis flow near a virtual electrode. The highest flow velocity exists on the surface at the edge of a virtual electrode. Owing to the symmetrical flow pattern, there exists a stagnant flow zone near the middle surface of a virtual electrode. This is where the nanoparticles are trapped.

The LACE mechanism is simulated using both the electrostatic and incompressible Navier Stoke's fluidic models on FEMLAB 3.0. A dc electrostatic model is chosen to

calculate the zeta potential, the tangential component of the electric field, and the slip velocity at the surface of the photoconductive layer. In the dc electrostatic simulation, the double layer capacitor layer is represented by a conductive layer with an equivalent electrical resistance at the operation frequency. Fig. 2 shows the vertical and tangential components of electric field in the liquid layer using the following parameters, double layer thickness: 10 nm, liquid conductivity: 10 mS/m, applied bias: 2 V. The impedance of the capacitor is calculated at 8 kHz. The photoconductivity in the a-Si:H layer is a Gaussian distribution with a full-width-at-half-maximum (FWHW) spot size of 30 μm and a peak conductivity of 0.2 mS/m. Fig. 2(a) shows that the vertical electric field is symmetric with respect to the center of the illumination spot and has a strong gradient near the surface. The tangential electric field on the surface is anti-symmetric and has it largest magnitude at the edge of a virtual electrode as shown in Fig. 2(b). The tangential electric field and the voltage across the capacitor layer, zeta potential, are extracted from the electrostatic model to calculate the slip velocity at the interface using Eq. (1). This slip velocity profile is used as the boundary condition to solve the incompressible Navier Stoke's equations for the flow pattern shown in Fig. 3.

In Fig. 3, this light induced flow circulates around the illumination spot with the highest velocity at the edge of a virtual electrode. In the center surface of the virtual electrode, there exists a stagnant zone where the flow speed is zero as shown in the inset in Fig. 3. Nanoparticles suspended in the medium near the virtual electrode are circulated to the edge of the virtual electrode by viscous fluidic force and swept into the stagnant zone.

IV. Experimental Results

Using LACE mechanism, we have created 31,000 traps across a 1.3 × 1 mm^2 area for trapping and transporting 2-μm beads in parallel using a DMD display. The illumination source is a red light-emitting diode (625 nm wavelength), and each light pixel uses 25 nW light power. Fig. 4 shows a small part of this trap array. Each trap is produced by a single DMD micromirror pixel. The spot size of each virtual electrode is 1.54 μm and the pitch is 8 μm. In Fig. 4(a), the particles are randomly distributed and not yet trapped by LACE. Within a second, these particles are swept into the bright spots by microfluidic vortices induced around virtual electrodes. The spot size of the virtual electrode is small enough that each trap only accommodates one particle. The un-trapped particles keep moving in the dark area until they are captured by an empty trap, as shown in Fig. 4(b). Two trapped particles can be combined together by projecting optical patterns with optical spots merging. The applied ac frequency is 1 kHz and the bias is 4 V_{pp}. The process from Fig. 4(a) to (c) takes less than 10 seconds. The same optical patterns can also be used to trap 1 μm beads individually. For particles with size smaller than 1 μm, multiple particles can be trapped in one optical spot.

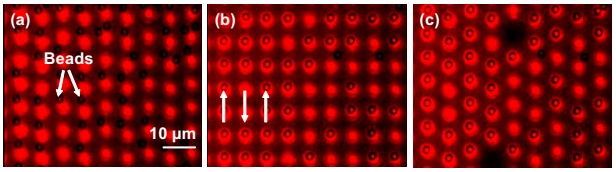

Fig. 4 Parallel trapping and transport of single 2-μm polystyrene beads. Each trap is produced by a single DMD pixel, and the pitch is 5 pixels. There are total 31,000 traps created on a 1.3 × 1 mm^2 area.

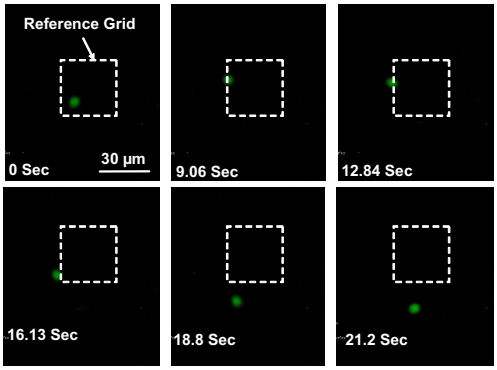

Fig. 5 LACE concentration of 200 nm fluorescent polystyrene particles using a 5-mW, 632 nm scanning laser beam. The diameter of the illuminating laser spot is 17.6 μm. The maximum transport speed is 7.6 μm/sec.

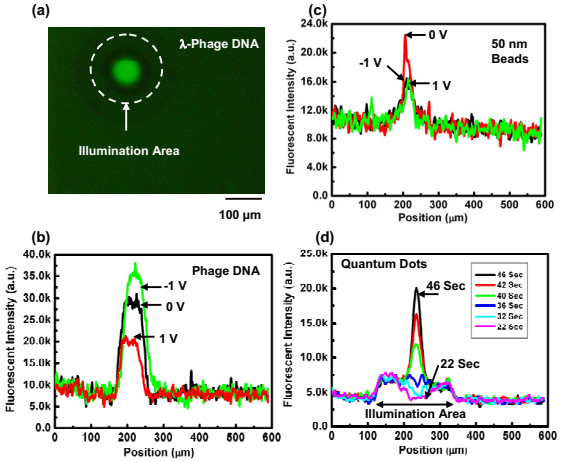

Fig. 6 LACE concentration using a circular virtual electrode patterned by partially closing the iris ring on an inverted microscope during fluorescent excitation. (a) Picture of concentrated phage DNA molecules. (b)(c) Effects of adding dc biases to perturb LACE concentration of λ-phage DNA and 50-nm carboxylated polystyrene beads. (d) Concentrating green fluorescent quantum dots.

Since light-patterned virtual electrodes can be continuously reconfigured on a featureless LACE device, this allows a light beam to concentrate and transport nanoparticles to any locations on a 2D surface without losing them. This is difficult

to achieve using physically patterned, digitized electrodes since the effective trapping range between nearby electrodes may not overlap, which results in lose of trapped particles during transportation. Fig. 5 demonstrates a continuous transportation of 200 nm fluorescent polystyrene beads on a LACE device using a 5 mW, 632 nm laser beam with a spot size of 17.6 μm, and a $6V_{pp}$, 1 kHz ac bias. The maximum transport speed is 7.6 μm/sec.

LACE concentration of nanoparticles can also be activated directly by the halogen or mercury lamps on a microscope. Fig. 6(a) shows the concentration of λ-phage DNA (Rockland Immunochemicals, Inc.) by patterning the blue fluorescent excitation illumination light with a partially closed iris ring on an inverted microscope. The illuminated spot size is around 200 μm. It takes less than 10 seconds to concentrate λ-phage DNA molecules to what is shown in Fig. 6(a). We have also demonstrated LACE trapping of other type of nanoparticles including quantum dots (Invitrogen Inc., Qdot 565 ITK™ amino (PEG) quantum dots, 15~20 nm size) and 50-nm carboxylated polystyrene beads (Polysciences Inc.) as shown in Fig. 6(c)(d). Both of them are focused to the center of the illuminated area. Adding a dc bias introduces extra electrophoretic forces during LACE concentration process, however they do not seem to be dominant within -1~1 volt dc bias range for trapping λ-phage DNA molecules and the negatively charged 50 nm polystyrene beads as shown in Fig. 6(b)(c).

V. CONCLUSION

We have demonstrated a novel light-actuated ac electroosmosis mechanism that allows patterning microfluidic vortices on a featureless, photoconductive, hydrogenated amorphous silicon coated glass substrate using optical images. These light-patterned vortices, together with the self-aligned strong electric field on the surface of virtual electrodes, can concentrate and transport a variety of micro- and nano-scale particles including 2-μm, 1-μm, 200-nm, and 50-nm polystyrene beads, λ-phage DNA molecules, and quantum dots. By integrating a DMD microdisplay, we can generate 31,000 microfluidic vortices on a 1.3×1 mm^2 area with each vortex individually addressed a single digital micromirror pixel.

LACE provides the concentration and transportation functions for manipulating nanoparticles. However, it does not provide immobilization functions in the current version. Some surface modification steps will be necessary to treat the amorphous silicon surface for immobilizing concentrated nanoparticles or molecules to pattern the surface. LACE has demonstrated several advantages over other techniques for nanoparticle manipulations. The light-patterned virtual electrodes can be easily reconfigured to transport concentrated nanoparticles continuously on a two-dimensional surface without losing them. The low light intensity requirement for virtual electrode excitation allows massively parallel manipulation of tens of thousands of LACE traps using a spatial light modulator.

VI. REFERENCES

Reference

[1] A. Ashkin, J. M. Dziedzic, J. E. Bjorkholm, and S. Chu, "Observation of a Single-Beam Gradient Force Optical Trap For Dielectric Particles," *Optics Letters,* vol. 11, pp. 288-290, May 1986.

[2] D. G. Grier, "A revolution in optical manipulation," *Nature,* vol. 424, pp. 810-816, Aug 14 2003.

[3] C. F. Chou, J. O. Tegenfeldt, O. Bakajin, S. S. Chan, E. C. Cox, N. Darnton, T. Duke, and R. H. Austin, "Electrodeless dielectrophoresis of single- and double-stranded DNA," *Biophysical Journal,* vol. 83, pp. 2170-2179, Oct 2002.

[4] T. B. Jones, *Electromechanics of particles*. New York: Cambridge University Press, 1995.

[5] P. Y. Chiou, A. T. Ohta, and M. C. Wu, "Massively parallel manipulation of single cells and microparticles using optical images," *Nature,* vol. 436, pp. 370-372, Jul 21 2005.

[6] B. G. Hosu, K. Jakab, P. Banki, F. I. Toth, and G. Forgacs, "Magnetic tweezers for intracellular applications," *Review Of Scientific Instruments,* vol. 74, pp. 4158-4163, Sep 2003.

[7] H. Lee, A. M. Purdon, and R. M. Westervelt, "Manipulation of biological cells using a microelectromagnet matrix," *Applied Physics Letters,* vol. 85, pp. 1063-1065, Aug 9 2004.

[8] P. K. Wong, C. Y. Chen, T. H. Wang, and C. M. Ho, "Electrokinetic bioprocessor for concentrating cells and molecules," *Analytical Chemistry,* vol. 76, pp. 6908-6914, Dec 2004.

[9] H. Daiguji, P. D. Yang, and A. Majumdar, "Ion transport in nanofluidic channels," *Nano Letters,* vol. 4, pp. 137-142, Jan 2004.

[10] M. Mpholo, C. G. Smith, and A. B. D. Brown, "Low voltage plug flow pumping using anisotropic electrode arrays," *Sensors and Actuators B-Chemical,* vol. 92, pp. 262-268, Jul 2003.

[11] R. B. M. Schasfoort, S. Schlautmann, L. Hendrikse, and A. van den Berg, "Field-effect flow control for microfabricated fluidic networks," *Science,* vol. 286, pp. 942-945, Oct 1999.

[12] J. Lyklema, *Fundamentals of Interface and Colloid Science* vol. 2. London: Academic Press, 1991.

[13] R. C. Hayward, D. A. Saville, and I. A. Aksay, "Electrophoretic assembly of colloidal crystals with optically tunable micropatterns," *Nature,* vol. 404, pp. 56-59, Mar 2 2000.

[14] A. Ramos, H. Morgan, N. G. Green, and A. Castellanos, "AC electric-field-induced fluid flow in microelectrodes," *Journal of Colloid and Interface Science,* vol. 217, pp. 420-422, Sep 1999.